ARTICLE OPEN

Check for updates

Mineral weathering by *Collimonas pratensis* PMB3(1) as a function of mineral properties, solution chemistry and carbon substrate

Laura Picard[1,2], Cintia Blanco Nouche[1,2], Carine Cochet[2], Marie-Pierre Turpault[2] and Stéphane Uroz[1,2]✉

While the role of mineral weathering (MWe) bacteria in nutrient cycling and plant growth promotion is established, our understanding of the molecular mechanisms involved and how their contribution to MWe varies according to the mineral properties and the environmental conditions remain poorly documented. In this study, we investigate how the type of mineral, the source of carbon and the buffering capacity of the medium impacted the effectiveness at weathering of the strain PMB3(1) of *Collimonas pratensis* and the molecular mechanisms involved. Using abiotic and biotic weathering tests, we characterised the weatherability of the different minerals considered (i.e., biotite, olivine, garnet, hematite, apatite). We reveal that the model PMB3(1) strain is able to weather all the minerals tested and that its effectiveness is related to the weatherability of each mineral in poorly buffered condition, but not in buffered condition. Using single and double mutants affected in their Glucose-Methanol-Choline oxidoreductase activity and/or the biosynthesis of siderophore, we identify which mechanism the strain PMB3(1) uses to weather minerals in each condition. Our results indicate that the effectiveness at weathering of bacteria depends more strongly on the environmental conditions (carbon source, buffering capacity) than on the mineral type.

npj Materials Degradation (2023)7:76 ; https://doi.org/10.1038/s41529-023-00396-9

INTRODUCTION

In temperate regions, forests are mostly developed on acidic, nutrient poor, and rocky soils, making trees to experience nutrient limitations. These ecosystems are also rarely amended, consequently, the access and recycling of nutrients represent key processes for tree growth and ecosystem functioning. Beside the nutrients recovered from atmospheric deposits and organic matter decomposition, minerals and rocks represent a non-negligible source of inorganic nutrients[1]. Through their degradation (i.e., mineral weathering, MWe), the nutritive elements (i.e. P, K, Mg, Ca, Fe…) contained in the crystal structure of minerals become available for living organisms. Minerals and MWe are consequently essential in nutrient poor soils where they significantly contribute to the replenishment of soil fertility and tree nutrition.

Mineral weathering is driven both by the properties of minerals (i.e., intrinsic factors) and the environmental conditions (i.e., extrinsic factors)[2,3]. The weatherability of minerals is firstly determined by their chemical composition, crystalline structure, and particle size/surface area[3,4]. Due to these characteristics, minerals and rocks can be classified according to their stability and their dissolution rate at particular pH. As a consequence, certain classes of minerals are more resistant (e.g., quartz) or easily weathered (e.g., apatite). The size is also an important parameter as the smaller particles have a higher surface area and are usually characterized by an increased dissolution than bigger particles[5]. The weatherability of minerals is also determined by the extrinsic factors, which can be divided into two categories. The first category corresponds to abiotic conditions occurring in its close vicinity (i.e., pH[6], buffering capacity, water availability and circulation[7], temperatures[8,9], frost-thawing events[10]). The second category corresponds to the action of living organisms. Indeed, plants and microorganisms can chemically contribute to mineral weathering, or physically through the pressure exerted on minerals by plant roots and fungal hyphae[11–14]. Key questions are to determine the relative contribution of biotic and abiotic processes to mineral weathering and how the conditions (e.g., vegetation cover, nutrient availability) determine this dissolution and the mechanisms engaged by the microorganisms.

In soil, the enrichment of effective mineral weathering microorganisms in the root vicinity (i.e., rhizosphere) has been largely documented, especially for bacteria. Such increase has been observed for different plants, but with variations according to the seasons, the species, and the soil fertility[15–17]. The nutritional requirements of plants and the soil properties have been proposed as the main factors determining the enrichment of effective MWe bacteria in the rhizosphere (i.e., rhizosphere effect). Noticeably, stronger enrichments have been reported in the rhizosphere of plants growing in nutrient-poor soils, conditions where plants also increase their root exudations[18,19]. Exudates represent important source of carbon substrates for bacteria living in the rhizosphere, but the type and concentration of the compounds contained in these exudates vary according to the plant species, the season and the presence of mycorrhizal fungi of the root system. In forest soils, glucose, mannitol, or trehalose are considered as the main carbohydrates and polyols available[20–24]. Noticeably, rhizosphere bacteria are usually more effective at metabolizing carbon substrates than bacteria from the surrounding bulk soil and present a higher effectiveness at weathering minerals[15–17,20]. Glucose is the C source providing the higher MWe effectiveness as compared to mannitol, trehalose, saccharose, galactose, xylose, mannose, maltose, cellobiose, arabinose…[25–29]. Such differences suggest a link between the MWe ability of bacteria, their ecology and their metabolism.

[1]Université de Lorraine, INRAE, UMR1136, Interactions Arbres-Microorganismes, Nancy, France. [2]INRAE, UR1138, Biogéochimie des Ecosystèmes Forestiers, Champenoux, France. ✉email: stephane.uroz@inrae.fr

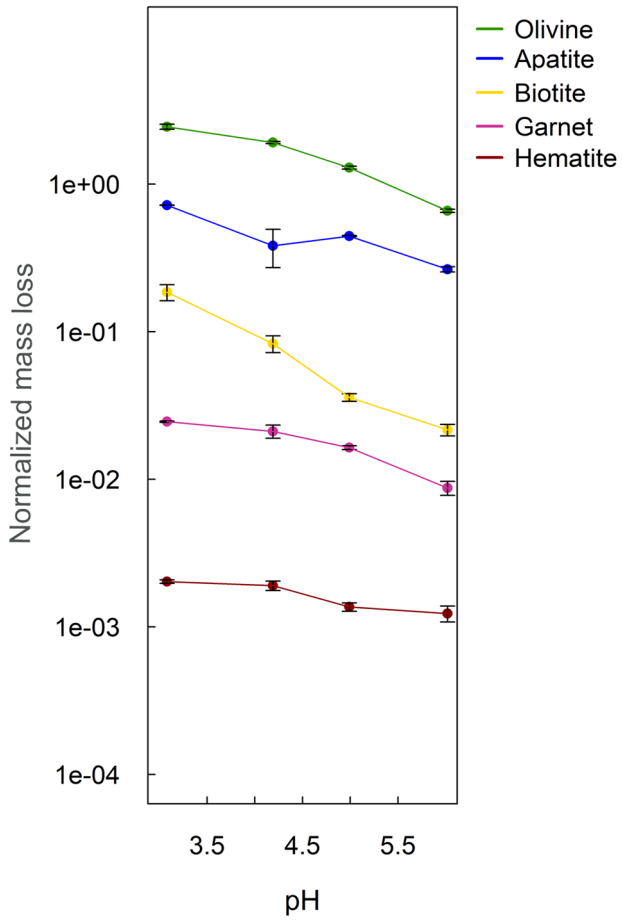

Fig. 1 Weatherability determination of the different minerals tested. The weatherability of each mineral was determined in acido-complexolysis conditions using a solution of 10 mM of citrate adjusted at pH 3.08, 4.19, 4.99, and 6.02 with HCl. Graphics represent the logarithm of the normalized mass loss for iron (released from olivine, biotite, garnet, and hematite) or calcium (released from apatite) according to pH of the different solutions tested. A similar experiment was done only using HCl (Supplementary Fig. 1). The error bars indicate standard deviations.

Effective MWe bacteria are known to operate using several mechanisms based on acidolysis (production of protons and acids) and complexolysis (production of chelators)[30–33]. The direct oxidative pathway is considered as the main mechanism used by bacteria to weather minerals through the action of glucose dehydrogenases (GDH). Indeed, many bacteria have the ability to bypass the classical glucose metabolism occurring in the cytoplasm to the direct oxidation of glucose occurring in the periplasm. The enzymes responsible are localized in the periplasm and convert glucose to gluconate and protons, leading to a local acidification of the surrounding environment of bacteria and to the dissolution of minerals[34–36]. As a consequence, the direct oxidative pathway produces little energy and biomass. To date, two types of GDH conferring a MWe ability have been reported: i) the GDH using the pyrroloquinoline quinone (PQQ) cofactor[37–43] and ii) the glucose/methanol/choline oxidoreductase (GMC) using the flavin adenine dinucleotide (FAD) cofactor[44]. Another important mechanism used by bacteria to directly or indirectly weather minerals is their ability to produce chelating molecules such as organic acids (e.g., oxalate) and siderophores. A lot of abiotic studies evidenced the action of chelating molecules such as siderophores or organic acids, but these studies did not consider metabolic adjustments and regulations occurring in microorganisms depending on nutrient availability (e.g., inhibition of siderophore production in the presence on iron)[33,45–47]. Comparatively, few studies addressed the question of how siderophore production contributed to mineral weathering in a cellular context. Based on the comparison of wild-type strains with their related mutants affected in siderophore production, pyoverdin and malleobactin have been identified as siderophores playing a key role in the weathering ability of *Pseudomonas* and *Collimonas*, respectively[48–50].

While MWe bacteria are well equipped to weather minerals, our understanding of the relative contribution of each mechanism used to weather, their potential combination, the environmental factors involved in the regulation of these mechanisms and the effect of the type of mineral remains limited. In this study, we investigated how the mineral type, the source of carbon and the buffering capacity of the medium impacted the effectiveness at weathering of the *Collimonas pratensis* strain PMB3(1) and the molecular mechanisms engaged. This model bacterial strain was chosen because of its high effectiveness at weathering[29,51] and the availability of mutants affected in their ability to acidify (i.e., GMC oxidoreductase[44], or to produce siderophore (i.e., malleobactin[50]). In this study, we completed the molecular work by creating a double mutant unable to acidify and to produce malleobactin. We coupled biotic and abiotic weathering in vitro tests to determine the effectiveness at weathering of the wild-type strain and its mutants, using i) different minerals (biotite, olivine, hematite, apatite, garnet, ii) two carbon sources (glucose and mannitol) and iii) two different media with high and low buffering capacity.

RESULTS

Mineral and weatherability characterization

The abiotic assay presented in Fig. 1 was designed to: (i) mimic acidocomplexolysis that can occur with bacteria, when both protons and organic acid with chelating properties are produced, and (ii) determine whether an effective MWe bacterial strain follow the trends observed in abiotic assays whatever the solution chemistry (data presented below). We decided to keep the conditions used in biotic assay (i.e. closed system, 7-days incubation, 150 rpm agitation) to compare with biotic data. The abiotic assays (Fig. 1) performed using citrate and varying pH conditions evidenced how acidocomplexolysis, a mechanism commonly used by bacteria to weather minerals, affected the dissolution of the different mineral considered. The same experiment without citrate was also performed to determine how acidolysis impacted mineral dissolution and differed from the acidocomplexolysis experiment (Supplementary Fig. 2A–D). The measures done of the iron released in solution clearly revealed the lowest concentrations for hematite (0.1 to 0.3 mg/L) and the highest for olivine (4 to more than 10 mg/L), showing how hematite is resistant. A specific focus done on the pH 3 condition, that corresponds to pH classically reached by bacteria during weathering, revealed that the higher normalized mass loss was observed for olivine with 2.45% (based on Fe), while apatite presented a lower normalized mass loss 0.72% (based on Ca). In contrast, biotite and garnet were the less weatherable with a normalized mass loss of 0.18% and 0.02% of Fe at pH 3, respectively. At last, our analyses revealed that hematite was the most recalcitrant mineral, with a normalized mass loss of 0.002% of Fe at pH 3. Together, our data both at the solution chemistry (Supplementary Fig. 2) and the normalized mass loss (Fig. 1) levels indicated that olivine and apatite were the most weatherable minerals among the five tested, confirming the data from the litterature[3,4]. Regarding the differences between acidocomplexolysis and acidolysis, our data confirm the higher impact of the acidocomplexolysis treatment, with a magnification level of 2 or more depending on the mineral considered. For most of the minerals tested (except hematite), the dissolution observed

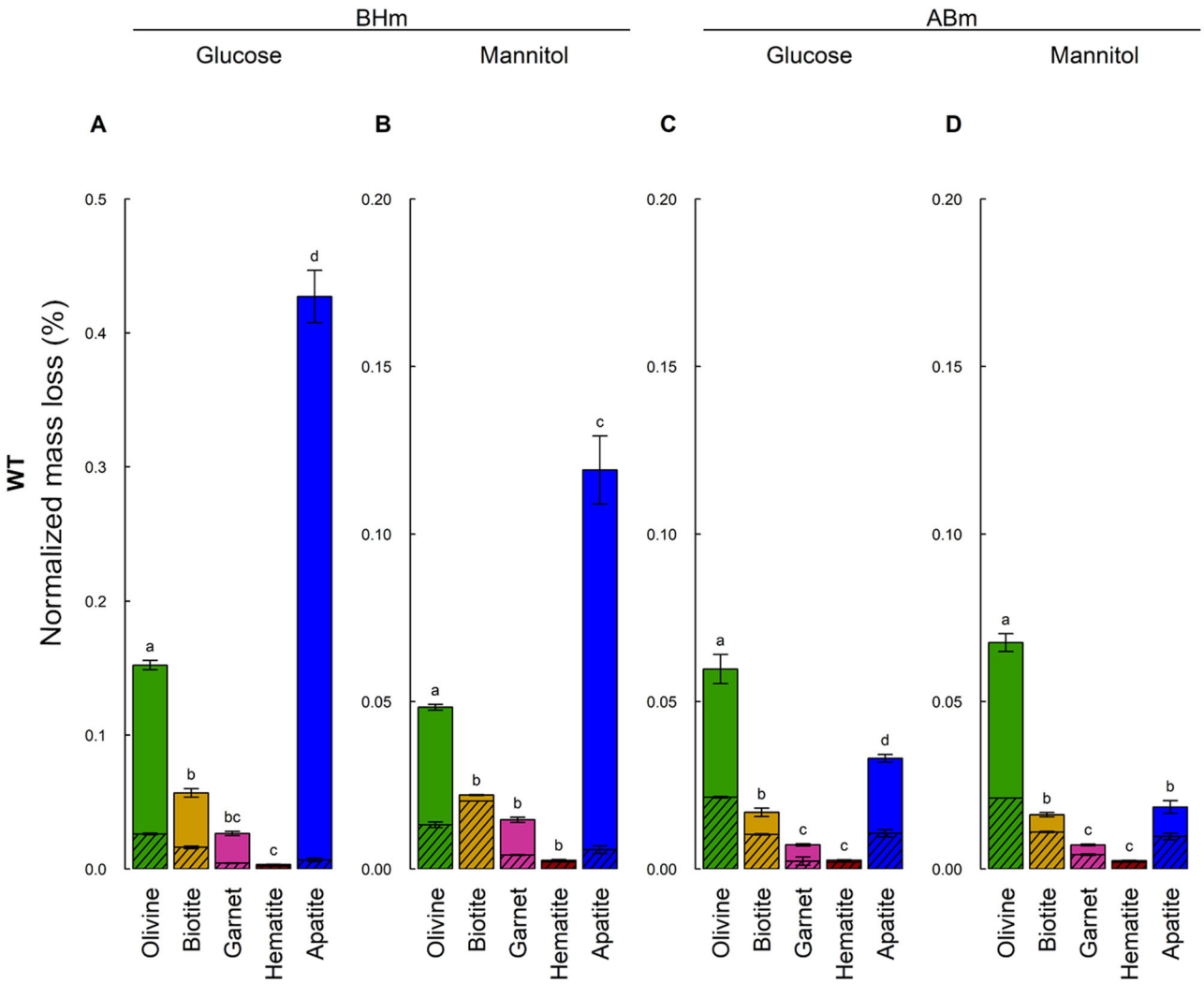

Fig. 2 Normalized mass losses of each mineral in presence of the strain *Collimonas pratensis* PMB3(1). The normalized mass loss for each mineral was calculated using the ratio of iron (for olivine, biotite, garnet and hematite) or calcium (for apatite) released in solution and the total quantity of this element (Fe or Ca) into the mineral structure. The active dissolution (full bar ; attributed to the action of the strain PMB3(1)) and the passive dissolution (hatched bar ; attributed to the abiotic dissolution in our experimental conditions) were evaluated in a BHm medium with low buffering capacity (**A** and **B**) or in ABm medium with high buffering capacity (**C** and **D**) supplemented with glucose (**A** and **C**) or mannitol (**B** and **D**) as sole carbon source. All treatments were done in triplicate. The error bars indicate standard deviations. For each treatment (BHm glucose, BHm mannitol, ABm glucose and ABm mannitol), different letters (a, b, c, d) above the bars indicate that the values are significantly different according to a one-factor (mineral) and TukeyHSD tests with *P*-value < 0.05. The error bars indicate standard deviations. For leagibility reason, the scale of the y axis was adjusted to the values presented.

tended to be magnified the more acidic was the pH (Fig. 1 and Supplementary Fig. 2).

Mineral type determines the effectiveness at weathering of strain PMB3(1)

The ability of strain PMB3(1) to weather different minerals was measured through incubation experiments in two types of medium and using two carbon sources. As the mineral considered varied in their chemical composition, we calculated the normalized mass loss in each condition based on the chemical element released in the solution to make comparable the data obtained for the different treatments. Such calculation was done to determine for which mineral (i.e., biotite, olivine, hematite, garnet and apatite) and which condition (i.e., low or high buffering capacity) the strain PMB3(1) was the most effective at weathering. Our analyses revealed higher normalized mass loss in the low buffered condition (i.e., BHm medium) than in high buffered condition (Fig. 2). For each culture condition, significant differences were observed between the different minerals incubated. In particular, the higher normalized mass losses were observed in the low buffering condition (BHm + glucose; Fig. 2A) for apatite (0.43%), olivine (0.15%), biotite (0.06%) and garnet (0.03%), while in the high buffering condition (ABm; Figure 2C, D) these values were lower (apatite, 0.018%; olivine, 0.06%; biotite, 0.016%; garnet, 0.008%). The impact of carbon source was clearly visible with a threefold reduction between glucose (Fig. 2A) and mannitol (Fig. 2B). In the high buffering condition (ABm), the impact of the carbon source was visible for apatite (0.03% with glucose vs 0.02% with mannitol) and negligible for the other. Hematite appeared very poorly weathered comparatively to all the other minerals considered by the strain PMB3(1) in all the conditions (Fig. 2).

Strain PMB3(1) uses different molecular mechanisms to weather minerals

Using different bioassays permitting to quantify the acidification ability and the production of siderophores, we characterized the

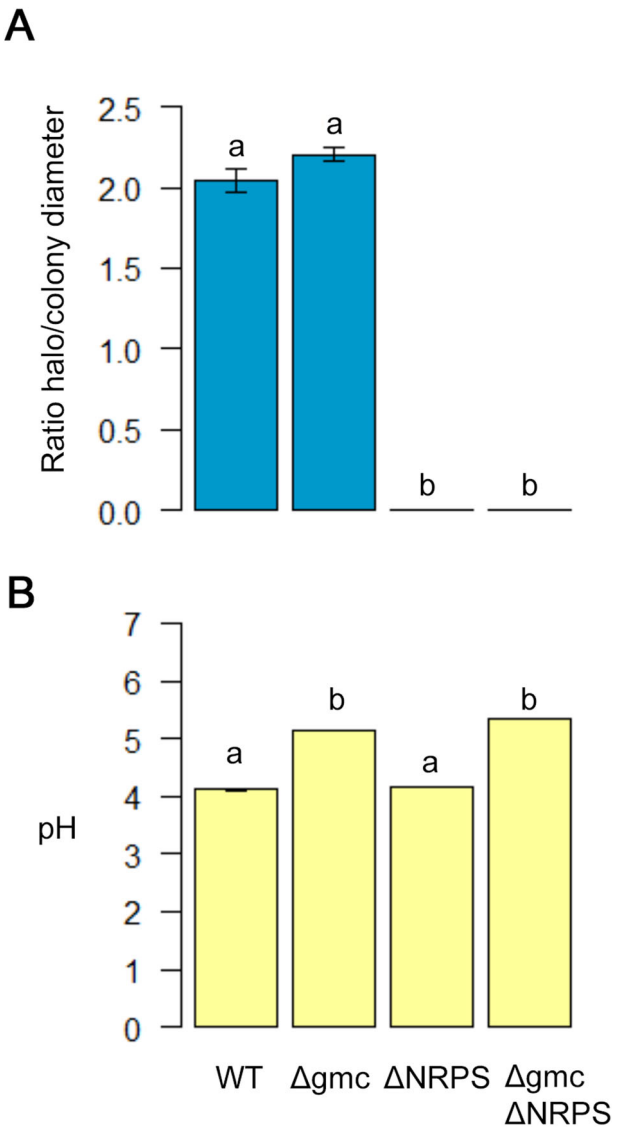

Fig. 3 Characterisation of weathering potential for *Collimonas pratensis* PMB3(1) and its mutants. A Chelating ability. The *Collimonas pratensis* strain PMB3(1) and its mutants (i.e. Δgmc, ΔNRPS and ΔgmcΔNRPS) were tested for the ability to mobilize iron from the Fe-CAS complex. The halo diameters and colony diameters on CAS agar plate were scored after 7-days incubation on solid medium. The Fig. 3A presents the ratio between halo diameter and colony diameter. **B** Acidifying ability. The same strains were tested for their ability to acidify the culture medium. After 2-days incubation in the TCP liquid medium the pH of the supernatant was scored. The error bars indicate standard deviations. For the ratio (halo /colony) diameter and the pH measurements, different letters above the bars indicate that the values are significantly different according to a one-factor (strain) ANOVA and TukeyHSD tests *P*-value < 0.05.

strain PMB3(1) and its mutants for their mineral weathering potential (Fig. 3). Our assays confirmed that the strain *Collimonas pratensis* PMB3(1) was able to acidify the medium from 6.5 to 4.1 in two days and to mobilize iron based on the CAS assay. In comparison, the mutant Δgmc (i.e., 25(10 F)) was significantly impacted in its ability to acidify the medium (from 6.5 to 5.1; $P < 0.05$), but not in its ability to mobilize iron (Δgmc = WT; 1.56 ± 0.1 cm of halo diameter; $P > 0.05$). The ΔNRPS mutant presented the same ability to acidify the medium than the WT strain (ΔNRPS = WT; pH from 6.5 to 4.2; $P > 0.05$), but was significantly impacted in its ability to mobilize iron (no halo formed). The double mutant ΔgmcΔNRPS was significantly impacted in both capacities (Fig. 3).

Contribution of the different molecular mechanisms to weather mineral according to the mineral type, the source of carbon and the solution chemistry

To identify the molecular mechanisms the most effective at weathering used by the strain PMB3(1) and their relative contribution according to the mineral type, the carbon source and the solution chemistry, we performed parallel weathering assays using the WT strain and its mutants varying a single parameter at a time. To evaluate the dissolution of minerals and the relative growth of the different bacterial strains, the concentration of chemical elements released in solution (and only present in the minerals) as well as the absorbance at 595 nm of the supernatant were measured (Fig. 4, Supplementary Figs. 3–7). Contrary to the data presented in Fig. 2, the dissolution data presented here (Fig. 4) were conserved as concentrations (mg/l) to permit to: (i) observation of the passive dissolution in the absence of bacteria, (ii) the real concentration of elements quantified in the medium in absence of mineral and bacteria, and iii) the comparison between the wild-type strain and its mutants. Noticeably, our bacterial growth data revealed higher cell biomass for the strain PMB3(1) in high buffering condition (i.e., the condition where the MWe effectiveness was the lowest) than in low buffering condition (i.e., the condition where the MWe effectiveness was the highest) (Supplementary Figure 3). Our analyses also revealed that the dissolution trend was very similar for the same mineral whatever the chemical element considered (Supplementary Figs. 3–6) and that the higher dissolution occurred in the low buffering condition. Consequently, and for legibility reasons, we only presented one element (Fe or Ca) for each mineral type to highlight the dissolution process according to the different conditions tested (Fig. 4).

In low buffering conditions (i.e., BHm medium), the higher dissolution was by far observed in the presence of glucose compared to mannitol, whatever the mineral type (increase of: 2× for biotite, 3× for olivine, 2× for garnet, and 3× for apatite) with the lower difference observed for hematite (increase of 1.4×). In the presence of glucose, the less effective strains at weathering were the mutants Δgmc and ΔgmcΔNRPS, both affected in their GMC oxidoreductase activity, for which lower acidification was observed. The same effect was observed whatever the type of mineral considered (Fig. 4A, E, I, M, Q). Interestingly, we were able to observe significant differences between the different strains (i.e., WT vs mutants) for hematite, while it was the less weatherable mineral considered as stated in Fig. 2. The concentrations of iron released in solution ranged from 0.3 (for the Δgmc mutant) to 0.5 mg/L (for the WT strain) for hematite (the less weatherable mineral) from 0.5 (for the Δgmc mutant) to 2.1 mg/L (for the WT strain) for olivine (one of the most weatherable mineral). For apatite, the concentrations of Ca released in solution ranged from 10 (for the Δgmc mutant) to 32 mg/l (for the WT strain). The single difference in terms of pH was observed for olivine, where a pH of 6.2 was measured after 7 days of incubation. For this particular mineral, a progressive increase in pH was observed after 2 days, corresponding to the formation of Mg carbonate (data not shown). In the presence of mannitol, the quantities of chemical elements released in solution were similar between the WT strain and the different mutants considered, but significantly higher than in the non-inoculated control (Fig. 4B, F, J, N, R).

In conditions with a stronger buffer (i.e., ABm medium), the quantities of chemical elements released from minerals in solution were by far less important than those observed in BHm medium (presented above), whatever the treatment considered. The concentrations of iron released in solution ranged from 0.2 (for

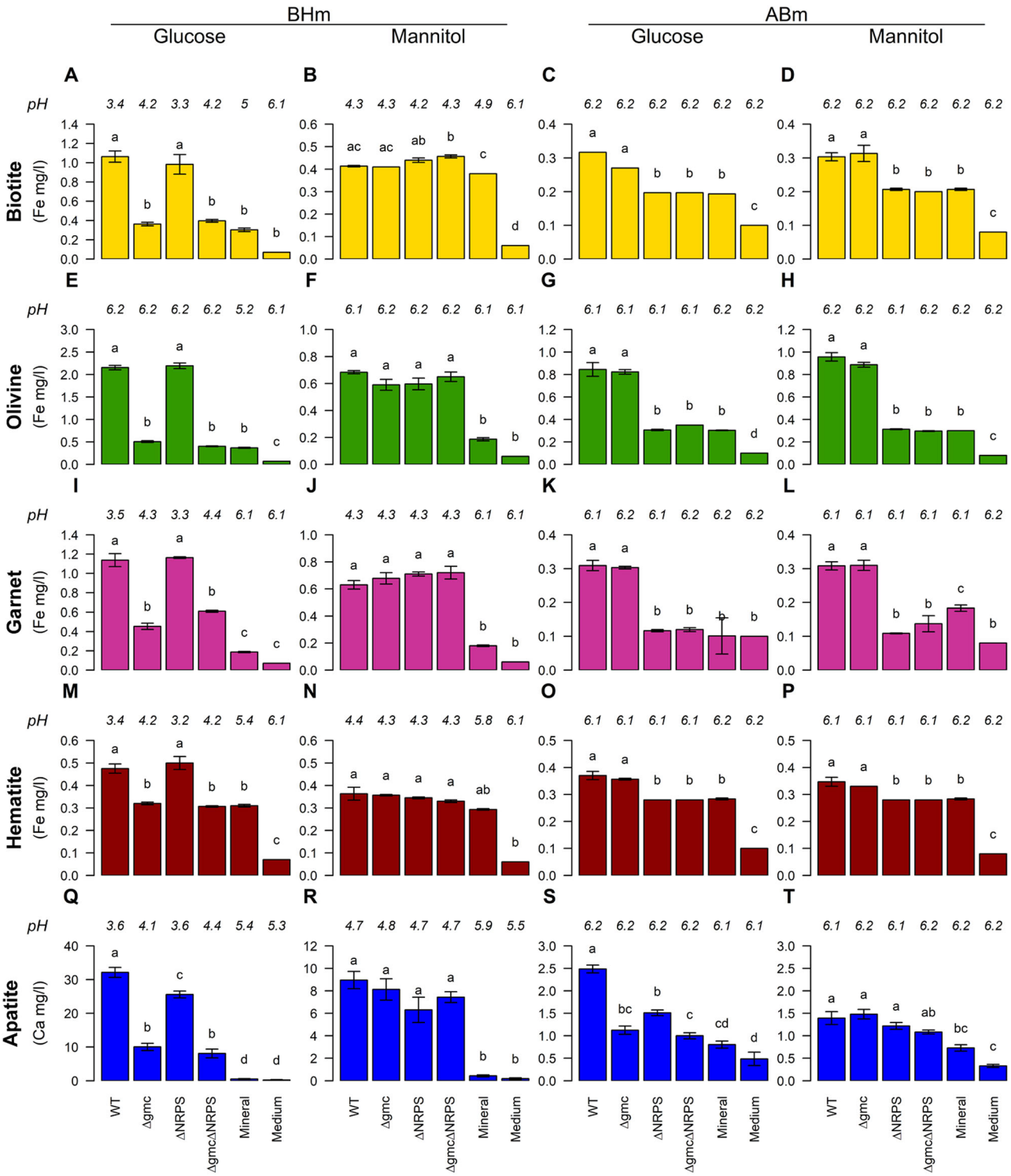

Fig. 4 Dissolution of different minerals by the strain PMB3(1) and its mutants (i.e. Δgmc, ΔNRPS and ΔgmcΔNRPS). The dissolution of minerals was determined by the concentration of (Fe or Ca) released from the minerals in the solution, after 7 days of incubation in a culture medium with low or high buffering capacity (BHm or ABm respectively) supplemented with glucose or mannitol (2 g/L). Non-inoculated controls with and without minerals allow to measure the passive dissolution and to validate the deficiency of the medium for the elements measured, respectively. The treatments are presented for each mineral considered as follows: for the biotite **A** BHm + Glucose; **B** BHm + Mannitol; **C** ABm + Glucose and **D** ABm + Mannitol; for the olivine **E** BHm + Glucose; **F** BHm + Mannitol; **G** ABm + Glucose and **H** ABm + Mannitol; for the garnet **I** BHm + Glucose; **J** BHm + Mannitol; **K** ABm + Glucose and **L** ABm + Mannitol; for the hematite **M** BHm + Glucose; **N** BHm + Mannitol; **O** ABm + Glucose and **P** ABm + Mannitol and for the apatite **Q** BHm + Glucose; **R** BHm + Mannitol; **S** ABm + Glucose and **T** ABm + Mannitol. The final pH of the medium is indicated in italics on the top of each graphic. Letters represent significant differences between the WT strain, mutants and non-inoculated controls ($P < 0.05$). The error bars indicate standard deviations. For leagibility reason, the scale of the y axis was adjusted to the values presented.

the ΔNRPS and ΔNRPSΔgmc mutants) to 0.3 mg/L (for the WT and Δgmc strains) for biotite and from 0.3 (for the ΔNRPS and ΔNRPSΔgmc mutants) to 0.8 mg/L (for the WT and Δgmc strains) for olivine. Although significant variations were observed between treatments, they remained weak. An important difference with the experiments done in low buffer conditions is that similar concentrations of Fe and pH values were observed in ABm medium for each mineral type in the presence of glucose or mannitol (Fig. 4C, D, G, H, K, L, O, P). The comparison of the WT strains and its mutants revealed that the less effective strains at weathering biotite, olivine, garnet, or hematite (i.e., iron-containing minerals) were the mutants ΔNRPS and ΔgmcΔNRPS as compared to the WT or the Δgmc strains, suggesting a key role of the siderophore (Fig. 4C, G, K, O). In contrast to the iron-containing minerals, a higher dissolution (based on the quantities of Ca in solution) was observed for apatite in the presence of glucose than mannitol in ABm medium for the WT strain. The pattern observed above (i.e., ΔNRPS and ΔgmcΔNRPS mutants the most affected) for the other minerals was not conserved for apatite (Fig. 4S, T). Indeed, in the presence of glucose, the WT strain significantly differed from the mutants and non-inoculated controls, while the mutants did not differ from the abiotic control with minerals. However, the concentrations of Ca remain very low compared to those obtained in the low buffering conditions. In the presence of mannitol, the inoculated treatments slightly differed from the abiotic treatment with mineral. Though the solution pH remains stable, we can not exclude that the strength of the TRIS buffer used was lower that the phosphate buffer usually used in the ABm medium, allowing to a higher dissolution in the presence of glucose. Noticeably, the liquid CAS test performed on the culture supernatants obtained in each mineral type revealed that the WT strain was capable of producing its siderophore. Our results suggest that in buffered conditions (i.e., ABm medium) the GMC-based mechanism (i.e., acidification) of strain PMB3(1) does not affect mineral stability, while the malleobactin-based mechanism (i.e., chelation) does but only on iron containing minerals.

DISCUSSION

In environmental conditions, the stability of the minerals and rocks strongly relies on their chemical properties and a combined action of biotic and abiotic processes. From abiotic experiments, it is well established that the mass loss and dissolution rates of a mineral are conditioned by (i) its physico-chemical properties (i.e., dissolution constant) and (ii) the experimental conditions (i.e., buffer condition, solution chemistry, pH, temperature…)[2,3]. In this sense, a same mineral incubated in solutions varying in pH or buffer can be characterized by different dissolution rates, as these conditions can accelerate or slow down the dissolution of different minerals. Such combinations of parameters (i.e., mineral type vs solution chemistry vs pH) have rarely been considered in biotic conditions. In this context, we can wonder how microorganisms can influence MWe according to nutrient availability and depending on the molecular mechanisms engaged. In this study, we combined abiotic and biotic dissolution assays to better understand whether the physico-chemical properties of minerals, the solution chemistry (i.e., buffering capacity) and carbon sources influenced the molecular mechanisms developed by bacteria to weather minerals and their effectiveness. To do so, we considered different types of minerals presenting the same surface area and incubated in the same experimental conditions.

The abiotic experiments done with solutions of citrate-HCl or only HCl in our study to mimic acidocomplexolysis and acidolysis permitted to classify the different minerals considered in our study according to their weatherability, using metabolites classically produced by plants and microorganisms (i.e., protons and/or citrate)[46,52–54]. Our analyses highlighted that olivine harboured the higher normalized mass loss as compared to hematite (normalized mass loss: Olivine>Apatite>Biotite>Garnet>Hematite). Although this classification fitted with previous abiotic characterization done on similar minerals[2,4,55,56], this order remains not so easy to explain as many factors can explain mineral weathering. From an abiotic perspective, this order is explained by the type of mineral (phosphate vs neosilicate vs phyllosilicate vs iron oxide), their chemical composition, their structure, and their reactivity/solubility in the aqueous conditions considered[2–6,47,49]. From a biotic perspective, microorganisms can impact mineral stability and the solution chemistry due to the nutritive content of the minerals, the quantity of chemical element absorbed and/or adsorbed in and on their cells and the affinity and stability of the chelating molecules with iron. In our case, the complex formation constants for malleobactin with iron remain unknown, limiting our conclusions. The biotic assays done with the strain PMB3(1) revealed that this strain was able to weather all the minerals considered as compared to the non-inoculated control. Until this study, this strain was only known for its ability to weather tricalcium phosphate, biotite and hematite[44,50,57]. Our results evidence that this strain has the ability to weather a broader range of minerals, which questions the relative (a)specificity of the mechanisms engaged according to the mineral type and their effectiveness at weathering. Noticeably, the normalized mass losses determined significantly differed depending on the mineral type, the initial solution chemistry (i.e., medium, pH) and the carbon source. The higher normalized mass losses obtained in low buffering condition suggest an important impact of acidification-related metabolites (e.g., protons, organic acids). Noticeably, this condition is also the one where the growth is the most limited, due to a preferential use of the direct oxidative pathway. In such condition, the different minerals followed the same order in term of normalized mass losses than those obtained in abiotic conditions (i.e., Apatite>Olivine>Biotite>Garnet>Hematite). In contrast, a different order was observed in condition with a high buffering capacity (Olivine>Biotite=Garnet>Hematite=Apatite), highlighting the strong impact of the buffering capacity of the medium and a potential change in the mechanisms used by the bacteria to interact and weather minerals. Noticeably, this condition is characterized by a higher growth of strain PMB3(1) compared to the low buffering capacity condition, evidencing a preferential use of the nutritive resources of the medium to produce cell biomass and siderophores. The differences of MWe effectiveness between the buffered and poorly buffered conditions suggest that the solution chemistry (i.e., the environmental conditions) plays an important role on the metabolic pathways and the molecular mechanisms engaged by MWe bacteria as well as their effectiveness[58–61].

While it is well established that bacteria adapt their physiology according to nutrient limitation and the carbon sources metabolized, our knowledge on their potential response to the presence of a mineral in their close environment or nutrient deficiency (e.g., K, Mg) is limited[62]. At the ecological level, the selective effect of minerals has been evidenced in various environments (e.g., aquifer, soil, rhizosphere), meaning that minerals are reactive interfaces and that the bacterial communities colonizing their surfaces (i.e., the mineralosphere) are adapted to this particular niche[63,64]. All these studies suggested that this selection/enrichment was attributed to the physico-chemical properties of those minerals, and especially their nutritive content (e.g., P, Mg, K, Fe released during mineral dissolution) and their reactivity (e.g., impact of the carbonate during calcite dissolution). Differences were not only visible in term of taxonomic distribution, but also in term of function. Indeed, global assays (i.e., BIOLOG and enzymatic tests) and MWe assays done on bacterial isolates revealed significant differences between communities, according to the type of minerals[64]. Noticeably differences were also observed according to the land cover, suggesting a link between the soil

properties, the plant derived carbon substrates and potentially the plant microbiota. At the physiological level, the response of bacteria interacting and/or weathering minerals has only been evidenced recently using transcriptomics and proteomics methods[58,65–67]. While the bacterial strains tested and the types of minerals differed, those studies highlighted that bacteria adapt to the presence of the type of mineral and the chemical element released and contribute to MWe. The challenge is now to go further than the simple reaction of the bacteria to the nutrients released by passive dissolution and to identify the mechanisms actively involved. Such developments should permit to better understand part of the discrepancy between the weathering of minerals observed in vitro and in field conditions.

From what it is currently known, the ability of bacteria to weather minerals strongly depends on a suite of mechanisms based on acidification, chelation, electron transfer, nutrient uptake or exopolysaccharide production, which relative roles in the MWe process and regulation remain unknown[59]. The strain *Collimonas pratensis* PMB3(1) used in our study is considered as very effective at weathering biotite. Its high effectiveness at weathering is partly linked to its ability to convert glucose to gluconic acid. The identification of the molecular mechanism and of the related genes permitted to identify the enzyme involved (i.e., GMC oxidoreductase) and to better understand the relative effect of the acidification produced by the strain PMB3(1) on minerals[44]. Detailed analysis and comparison with other studies revealed that in nutrient-poor condition, strain PMB3(1) is capable of using a particular metabolic pathway (i.e., the direct oxidative pathway of glucose) which leads to a low biomass and energy production, but a high quantity of protons released in the extracellular environment[60,61]. Interestingly, the same strain appeared also capable of producing a siderophore, identified as malleobactin, in Fe-limiting conditions[50]. A mutant affected in the production of this siderophore appeared non-effective at weathering hematite. However, the two mechanisms (i.e., acidification and siderophore production) have not been evidenced in the same experimental conditions (weak vs strong buffer) nor on the same type of mineral (biotite vs hematite)[44,50]. While many bacterial strains have been reported to have one or both activity[29,57], the relative contribution of each mechanism and/or their potential synergistic effect has rarely been demonstrated. Abiotic experiments using organic acids and siderophores used alone or in combination in presence of a mineral showed synergistic effect, dependent on the pH of the solution[56]. However abiotic experiments can not consider physiological adjustments and regulations operated by bacteria during the mineral-bacteria interactions and the MWe process. By testing single or double mutants in this study, we clearly evidenced by which preferential mechanism the strain PMB3(1) is capable of mobilizing nutrients from minerals, with an effectiveness strongly dependent on the mineral type and the solution chemistry. The use of the double mutant ΔgmcΔNRPS (i.e., GMC and malleobactin defective) also highlighted that there was no cumulative/synergic effect of the two mechanisms in our experimental conditions.

In the buffered condition (i.e., ABm medium) the phenomena observed differed. In such condition, chelation appeared as the main mechanism associated to the effectiveness of the strain PMB3(1) at weathering most of the minerals tested. Malleobactin production was detected for both glucose and mannitol amended media with no quantitative effect. The pH of the solution remained stable, evidencing the importance of the buffering capacity of the medium on the bacterial MWe and the MWe mechanisms engaged. The role of siderophore in weathering of iron-containing minerals has been evidenced for various bacterial strains[58,68–71], but their action on iron-free minerals such as apatite is poorly documented. The experiment done in our study with apatite (an iron-free mineral) permitted to highlight a high production of malleobactin. Although apatite is iron-free mineral, it contains some elements that could interact with the malleobactin as manganese[72] or with traces of rare earth elements (Cerium)[73] and influence the dissolution of apatite. Our analyses did not reveal any effect on the dissolution of apatite as stated by the calcium content measured in the solution of both the WT strain and malleobactin-defective mutant in presence of mannitol as sole carbon source.

The conclusions of our study were however obtained from a single time point. This is an important limitation, as bacterial physiology and geochemical reactions are dynamic processes. One can consider that different results would have been obtained after a shorter or longer incubation times or by considering an open-system flow microcosm. Indeed, the content of carbon remaining for bacterial metabolism or the solution saturation probably change across time. Kinetic experiment would provide a complementary view of the dissolution process in presence of the different bacterial strains. Noticeably, partial results (only on iron) obtained after 3-days incubation in our experiment revealed a similar trend than after 7 days between the different strains and the different treatments (i.e., carbon source, type of medium)(data not shown). Knowing these limitations, our data suggest that in natural conditions effective MWe bacteria can adapt their physiology and switch from an acidification to a chelation-based MWe behavior and vice versa. Interestingly, similar conclusions were obtained by Valbi et al.[74] considering the dissolution of potash-lime silicate glasses in presence of a strain of *Pseudomonas putida*. The authors revealed a first phase of dissolution based on an acidifying mechanism and a late stage based on chelating mechanism[74]. From our observations and the data from the literature[58,59,65,75,76], a model can be proposed according to the environmental conditions. In low buffering conditions and until final consumption of a carbon substrate allowing to moderate to high acidification (e.g., glucose), siderophore production is reduced due to a lower growth in acidic conditions and can be even inhibited depending on nutrient availability. Indeed, the nutrients released in the solution (including Fe) during the MWe process and the higher iron solubility at low pH inhibit the production of malleobactin by the strain PMB3(1). Such regulation of the siderophore production according to the iron availability is a well-known regulation mechanism in bacteria. In low buffering conditions, MWe is consequently mainly based on the production of protons and gluconic acid by the strain PMB3(1). These protons are partially consumed by the mineral surfaces in exchange of the nutrients released (e.g., K, Mg, P) and can change the buffering capacity of the solution. These nutrients are then absorbed by the microorganisms (i.e., uptake mechanisms) and/or subjected to precipitation/adsorption events allowing to the formation of secondary minerals (e.g., Fe oxides and hydroxides, Mg carbonate)[75]. The decrease of available iron for different reasons listed above can promote siderophore production. This is what probably occurs in high buffering conditions (e.g., carbonate rich environment or presence of a buffer). In such condition, protons and organic acid coming from the carbon metabolisms are neutralized and do not act on mineral surfaces (or poorly), while the siderophore can be produced and contribute to MWe. In this second case, MWe is mainly based on the production of malleobactin by the strain PMB3(1).

To conclude, our study provides a better understanding on interconnection between mineralogy, bacterial physiology and environmental conditions. By testing different mineral types, we highlighted that the strain *Collimonas pratensis* PMB3(1) is effective at weathering a broad range of minerals and particularly using glucose as carbon substrate (Fig. 5). Noticeably, the solution chemistry plays an important role on the molecular mechanisms used by this strain to weather minerals, with acidification the most effective mechanism at weathering in low buffering condition and chelation the most effective mechanism in high buffering conditions. While a synergistic effect has been proposed based

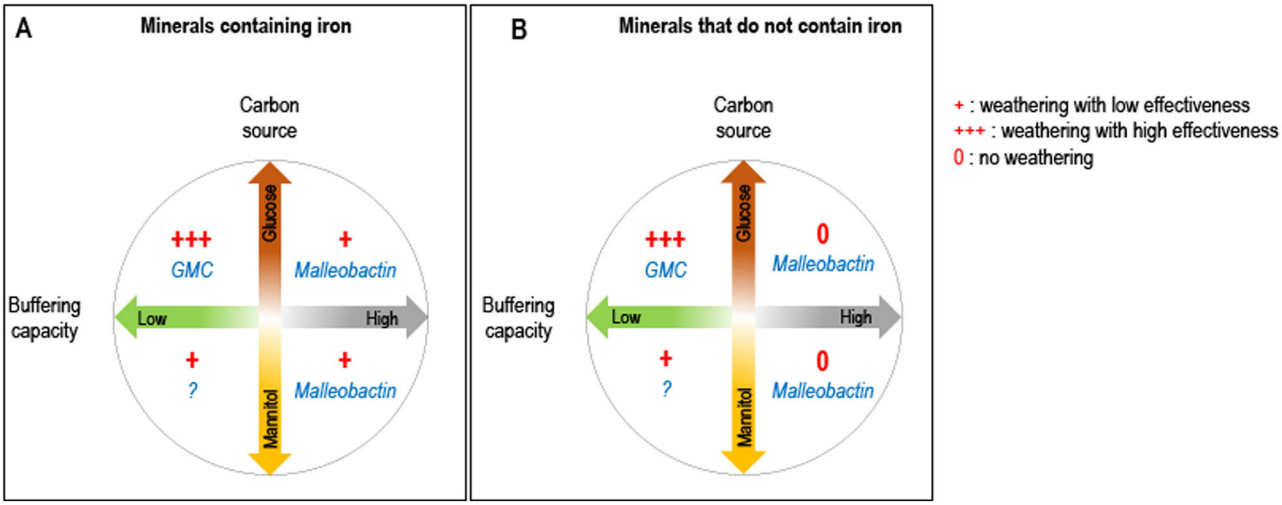

Fig. 5 Adjustments of the molecular mechanisms used by the strain *Collimonas pratensis* PMB3(1) to weather mineral according to the solution chemistry, the source of carbon and the type of mineral. The strain PMB3(1) is known to weather minerals using acidification and chelation related mechanisms, but their activation and effectiveness strongly depend on the solution chemistry (i.e., buffering capacity of the medium, the source of carbon and iron availability). The hypothetical model presented here illustrates the different adjustments done by the strain PMB3(1) based on the different experimentations done in the study and from the literature. **A** presents the mechanisms preferentially used by the strain PMB3(1) to weather minerals containing iron in their structure. **B** presents the mechanisms preferentially used by the strain PMB3(1) to weather minerals that do not contain iron in their structure. In each condition, the mechanisms involved are presented as follows: (i) GMC : GMC oxidoreductase allowing to the conversion of glucose to gluconic acid and protons, (ii) Malleobactin: siderophore involved in the mobilization of iron and iii) ? : unknown molecular mechanism(s). For all the minerals: i) In low buffered condition supplemented with glucose (BHm + glucose), the model strain mainly weather minerals by acidolysis through its GMC oxidoreductase activity. In this condition, the dissolution is the higher (+++) compared to the other conditions. (ii) In the same medium supplemented with mannitol (BHm + mannitol), the dissolution is quantifiable, but low (+). The molecular mechanisms used by the strain PMB3(1) to allow this low dissolution remain unknown (?) in this specific case. The strain PMB3(1) can also use complexolysis mechanisms, but the production of siderophore depends on the absence or low concentration of iron available in the solution. In low buffered condition and whatever the source of carbon, malleobactin is not produced due to the release of iron in solution by the GMC activity. In contrast, in highly buffered condition and whatever the source of carbon, the acidity produced by the GMC activity is neutralized, the malleobactin is consequently produced. The dissolution observed in such condition is mostly attributed to the action of the malleobactin. This mechanism is however less effective at weathering than acidolysis (+). For minerals devoid of iron, no active dissolution occurs in highly buffered medium (0), while malleobactin is produced.

on abiotic experiments or through the addition of organic acids or siderophore in cultures, our results reveal that whether a synergy exists between the two mechanisms, it can not be in a real time, but in a sequential way. Further experiments will be necessary to validate this assumption. Last, our results provide complementary information on why the magnitude of weathering strongly vary between in vitro and field conditions.

METHODS

Mineral material

All minerals used in this study are natural crystals bought to different companies (Table 1A). Five different minerals: apatite, biotite, olivine, hematite and garnet were selected. These minerals have been considered because of their occurrence in soil and their chemical composition. Indeed, these minerals are composed of different nutritive elements essential for plant growth (i.e., K, Mg, P, Ca, Fe…). They were also chosen because of their contrasting physico-chemical properties and weatherability. Their chemical composition and structural composition were measured or determined by inductively coupled plasma–atomic emission spectroscopy (ICP-AES), after alkaline fusion with $LiBO_2$ and dissolution in HNO_3 (Table 1A and B). The DRX analysis was used to confirm the purity of minerals. For each mineral, particles were crushed and size calibrated to obtain 200 to 500 µm grains according to Calvaruso et al.[77]. Briefly, for each mineral type considered, we selected manually the purest crystals. After some pre-treatments (see below) to remove impurities, the minerals were crushed, dry-sieved to remove most fine particles, washed, ultrasonically (2 min, three times at 100 V) treated to remove the remaining fine particles and water-sieved to obtain size-calibrated particles between 200 and 500 µm. The particles were then dried at 30 °C before any manipulation. Manual sorting under the binocular was done and particles with impurities were carried out. For biotite the pre-treatment consisted in the manual removal of calcite impurities or iron oxyhydroxides, while it was done with CBD (citrate-bicarbonate-dithionite) treatment for apatite.

Bacterial strains and growth media

The experiments presented in this study were done using the model *Collimonas pratensis* strain PMB3(1)[51,78] and three different mutants (Supplementary Table 1). Two mutants have been generated and characterized in previous studies. The first mutant Δgmc (previously named 25(10 F) in Picard et al.[44]) non-effective at weathering is mutated on the *gdhC* gene, which codes for the cytochrome subunit of a GMC oxidoreductase[44]. The second mutant ΔNRPS non-effective at weathering is mutated on the *mbaA* gene, which codes for a non-ribosomal peptide synthetase (NRPS) that is responsible of the biosynthesis of malleobactin[50]. The third mutant corresponds to a double mutant ΔgmcΔNRPS obtained in this study by mutating the *mbaA* gene in the mutant Δgmc, following the procedure described in Picard et al. 2022[50]. The media used were Luria-Bertani (LB), AB medium (AB[79]) and a modified version of the AB medium (ABm) and Bushnell-Haas (BHm) devoid of iron medium[51]. The ABm minimal (ABm) medium was supplemented with mannitol or glucose (2 g/L final concentration) as carbon source. Its composition (g/L) is: NH_4Cl, 1; $MgSO_4,7H_2O$, 0.3; KCl,0.15; $CaCl_2$, $2H_2O$, 0.0033; KH_2PO_4, 3; $Na_2PO_4,2H_2O$, 1.15, adjusted at pH 7. For the apatite weathering experiments done in ABm, the phosphate buffers were replaced

Table 1. Characteristics of each mineral considered.

A. Chemical formula of each mineral

Mineral	Origin	Provider	Chemical formula
Biotite	Bancroft, Canada	Association des géologues, Canada	(Si_3Al_1) $(Fe^{3+}{}_{0.12}Fe^{2+}{}_{0.61}Mg_{2.06}Mn_{0.02}Ti_{0.13})$ $K_{0.88}Na_{0.06}O_{10}$ $(OH_{0.98}F_{1.02})$
Apatite	Brasil	Krantz (Rheinisches Mineralien-Konor), Germany	$Ca_{9.52}Na_{0.08}Ce_{0.04}Fe_{0.01}Mg_{0.01}Sr_{0.01}P_{5.90}O_{23.62}F_{1.57}OH_{0.81}$
Olivine	Madagascar	Compagnie de Madagascar, France	$(Mg_{1.82}Fe^{2+}{}_{0.19})(Si_{0.99}O_4)$
Hematite	Brasil	LP Minerais do Brasil ltda.,Brasil	Fe_2O_3
Garnet	Brasil	LP Minerais do Brasil ltda.,Brasil	$Al_{1.96}Mg_{1.82}Fe^{2+}{}_{1.85}Mn_{0.80(}Si_{3.01}O_{12})$

B. Major elemental composition of each mineral (in g/kg)

	Chemical composition									
	SiO_2	Al_2O_3	Fe_2O_3	FeO	MnO	MgO	CaO	Na_2O	K_2O	P_2O_5
Biotite	410.1	109.0	22.1	100.5	2.7	189.0	0.00	4.1	94.6	0.00
Olivine	404.1	0.00	/	91.0	1.2	496.7	0.8	/	/	/
Garnet	374.5	206.3	0.00	275.5	117.1	24.5	6.4	/	/	2.0
Hematite	1.8	1.6	993.0	/	0.4	1.0	/	/	/	/
Apatite	8.1	1.0	1.0	/	0.3	0.2	526.4	2.3	0.00	412.6

by Tris(hydroxymethyl)aminomethane, 6 g/L and $Na_2PO_4{,}2H_2O$ was added at 10 mg/L. The BHm medium was supplemented with mannitol or glucose (2 g/L final concentration) as carbon source. Its composition (g/L) is: KCl, 0.020; MgSO4·$7H_2O$, 0.150; $NaH_2PO_4{\cdot}2H_2O$, 0.080; $Na_2HPO_4{\cdot}2H_2O$, 0.090; $(NH_4)_2SO_4$, 0.065; KNO_3, 0.100; and $CaCl_2$, 0.020, adjusted at pH 6.5. For the apatite weathering experiments done in BHm, the phosphate buffers were removed and $Na_2PO_4.2H_2O$ was added at 10 mg/L. All strains were grown at 25 °C. Antibiotics were added to the media only for the production of the inoculum at the following final concentrations: tetracycline 10 µg/mL and/or gentamycin 20 µg/mL.

Preparation of bacterial inoculum

For each assay presented below, the wild type (WT) strain PMB3(1) and the mutant strains (i.e., Δgmc, ΔNRPS, ΔgmcΔNRPS) were recovered from glycerol stock (−80 °C) and grown on solid ABm medium with mannitol (2 g/L), amended with gentamycin for the ΔNRPS mutant, tetracycline for the Δgmc mutant and both antibiotics for the ΔgmcΔNRPS mutant. After a 2-day incubation at 25 °C, one colony of each strain was inoculated in liquid AB medium (10 mL) supplemented with mannitol (2 g/L) and antibiotics (as described above) and incubated for 2 days at 25 °C under 200 rpm agitation. The cultures were then centrifuged at 8,000 g for 15 min at 10 °C and the pellet was washed twice with 5 ml of sterile Milli-Q water to eliminate all culture medium and antibiotic traces. The pellet was recovered in 5 ml of sterile Milli-Q water. To control the quantity of cells inoculated, the optical density (OD) was measured at 595 nm and cell suspensions were adjusted at 0.90 ± 0.03.

Phenotypic characterisation : Solution acidification assay

Ten microliters of calibrated inoculum were inoculated in 190 µL of liquid TriCalcium Phosphate (TCP) medium (without $Ca_3(PO_4)_2$). After 3 days of incubation, the microplate was centrifuged at 5000 g, 15 min at 4 °C. A total of 180 µL of supernatant was sampled and added to 20 µL of bromocresol green (1 g/L). The absorbance at 595 nm was measured and the data were transformed in pH according to Uroz et al.[51].

Phenotypic characterisation: Siderophore activity

The Chrome Azurol S (CAS) assay was performed according to Schwyn and Neilands[80]. A volume of 5 µL of bacterial inoculum of each strain tested was inoculated on CAS agar plates and incubated at 25 °C for 3 days. The diameters of both the yellow halo formed around the colony and/or of the colony were scored to determine siderophore production and the growth of the different strains tested.

Experimental design of the abiotic and biotic Mineral weathering assays

To evaluate mineral dissolution in abiotic or biotic conditions, the same experimental design was performed (Supplementary Fig. 1). A closed system was used with glass tubes washed with hydrochloric acid (HCl, 3.6%) and rinsed thrice in MilliQ water. One hundred milligrams of minerals (i.e., apatite, biotite, olivine, hematite, or garnet) were added to each tube. Then, they were sterilised by autoclaving at 121 °C. Five milliliters of the sterile solutions or media ± bacterial inoculum (described below) were added to each tube in sterile conditions. Tubes were incubated in shaking incubators at 25 °C, 150 rpm for 7 days. All samples were treated in triplicate for statistical analysis.

Abiotic mineral weathering assay

To evaluate the weatherability of each of the five minerals, a solution of HCl and 10 mM citrate was used to mimic acido-complexolysis or only acidolysis in absence of citrate. Such combination was considered because bacteria are known to produce several metabolites (e.g., protons and organic acids) that jointly act on minerals. The quantity of HCl was adjusted to obtain the following pH values: 3.15; 4.15; 5.01; 5.22. These solutions were used to solubilize citrate at a final concentration of 10 mM each. Then the pH of each solution was readjusted to obtain solutions with a final pH value of: 3.08; 4.19; 4.99; 6.02 with NaOH (2 N). All these solutions were autoclaved at 121 °C and the pH of each solution was verified after the sterilisation process.

After the incubation with minerals (described above), the solutions were then separated from the mineral particles and filtered at 0.22 µm and stored at −20 °C for further analysis. The concentration of chemical elements released from minerals (Al, Ca, Mg, Fe, Mn, and P) was measured by inductively coupled plasma-

atomic emission spectrometry (700 Series ICP-AES, Agilent Technologies).

Biotic mineral weathering assay

Iron-deprived version of the ABm and BHm media were used for the weathering assays done with biotite, olivine, hematite, and garnet, to permit following mineral weathering through Fe measurement (Supplementary Figs. 4–6). The ABm medium was used because of its high buffering capacity, which strongly limits acidification, but permits complexolysis. In contrast, the BHm medium has a low buffering capacity that does not limit acidification. To investigate the impact of the carbon source on the MWe ability, both media were supplemented by either glucose or mannitol to a final concentration of 2 g/L. Glucose was chosen for its involvement in the direct oxidative pathway, leading to the production of protons and gluconic acid. Mannitol was chosen because it is effectively metabolized by the strain PMB3(1) and allows a good growth, but through a moderately-acidifying pathway. For apatite, the BHm and ABm media were adapted by removing calcium and reducing phosphorus content to permit to follow mineral weathering through Ca and P measurements (see composition of media in Supplementary Table 2). Preliminary experiments demonstrated that a minimal amount of P was necessary to allow bacterial growth. In this context, 10 mg/l of Na_2HPO_4, $2H_2O$, corresponding to 1.7 mg of P, were added to modified ABm and BHm media. To maintain a buffering capacity in the ABm medium, the phosphate buffer was replaced by a TRIS buffer (50 mM).

The same procedure described above was used. The tubes containing or not 100 mg of minerals (i.e., apatite, biotite, olivine, hematite, and garnet) were loaded with 4.5 mL of medium (ABm or BHm with glucose or mannitol) and 500 µL of bacterial inoculum (i.e., WT; Δgmc; ΔNRPS and ΔgmcΔNRPS strains). Non-inoculated media with and without minerals were used as controls. After 7 days of incubation, 200 µL of culture were sampled and distributed in a 96-wells microplate, the absorbance at 595 nm was measured to determine bacterial growth. Then, the cultures were centrifuged at 8,000 g and the supernatants were filtered at 0.22 µm and stored at −20 °C for further analyses. The concentration of chemical elements released from minerals (Al, Ca, Mg, Fe, Mn, and P) in each sample was measured by inductively coupled plasma-atomic emission spectrometry (700 Series ICP-AES, Agilent Technologies). In addition the iron content and the pH of each sample was determined using the ferrospectral and bromocresol green methods according to Uroz et al.[51]. The same culture supernatant was also used to measure siderophore production with the liquid CAS assay. Briefly, 100 µL of liquid CAS were mixed with 100 µL of supernatant in a 96-wells microplate. After 1 h incubation at room temperature in the dark, OD at 655 nm was measured. A decrease of absorbance corresponds to a change from blue to yellow when a siderophore is present.

Normalized mass loss calculation

To allow the comparison of the data obtained from the different minerals and the different media, the normalized mass losses (NML) were calculated using the chemical elements released from minerals into the solution. Only the chemical elements missing in the culture medium or the containers (glass tubes contain silicium) and contained into the minerals tested were considered as weathering markers. Concretely, we considered: (i) for biotite: Fe, Mg, Al ; (ii) for olivine: Fe, Mg; (iii) for garnet: Fe, Mg, Al, Mn; (iv) for hematite: Fe; and (v) for apatite Ca. For each chemical element, the normalized mass loss was obtained by using the formula: NML=Sx100/TM, where S corresponds to the quantity of chemical element contained in the solution (in the 5 mL) and TM corresponds to the total mass of this chemical element contained in the crystalline structure of the mineral considered. As the normalized mass losses obtained for each element gave similar trend for the same mineral, we decided for legibility reasons to only present normalized mass losses based on iron or calcium. The details of the different chemical elements (i.e., Fe, Al, Mg, Mn, Ca) measured in solution for each type of mineral are presented in the supplementary figures (Supplementary Figs. 4–7).

Statistical analyses

Statistical analyses were performed in R software. Data shown were means of independent triplicates. Differences between the sample's means were analyzed by ANOVA and Tukey HSD tests with P-value < 0.05. Means are presented with standard deviations and the presence of different letters (a, b, c, d) above the bars indicate that the values are significantly different.

DATA AVAILABILITY

All data needed to evaluate the conclusions in the paper are presented in the paper or in the supplementary files.

Received: 17 April 2023; Accepted: 14 September 2023;
Published online: 23 September 2023

REFERENCES

1. Ranger, J. & Turpault, M.-P. Input–output nutrient budgets as a diagnostic tool for sustainable forest management. *Ecol. Manag.* **122**, 139–154 (1999).
2. White, A. F. & Buss, H. L. Natural weathering rates of silicate minerals. in *Treatise on Geochemistry* 115–155 (Elsevier, 2014).
3. Bray, A. W. et al. The effect of pH, grain size, and organic ligands on biotite weathering rates. *Geochim. Cosmochim. Acta* **164**, 127–145 (2015).
4. Brantley, S. L. Kinetics of mineral dissolution. in *Kinetics of water-rock interaction* (eds. Brantley, S. L., Kubicki, J. D. & White, A. F.) 151–210 (Springer, 2008).
5. Dehner, C. A., Barton, L., Maurice, P. A. & DuBois, J. L. Size-dependent bioavailability of hematite (α-Fe_2O_3) nanoparticles to a common aerobic bacterium. *Environ. Sci. Technol.* **45**, 977–983 (2011).
6. Malmström, M. & Banwart, S. Biotite dissolution at 25 °C: the pH dependence of dissolution rate and stoichiometry. *Geochim. Cosmochim. Acta* **61**, 2779–2799 (1997).
7. Hilley, G. E., Chamberlain, C. P., Moon, S., Porder, S. & Willett, S. D. Competition between erosion and reaction kinetics in controlling silicate-weathering rates. *Earth Planet. Sci. Lett.* **293**, 191–199 (2010).
8. Bahr, H.-A., Fischer, G. & Weiss, H.-J. Thermal-shock crack patterns explained by single and multiple crack propagation. *J. Mater. Sci.* **21**, 2716–2720 (1986).
9. Hall, K., Guglielmin, M. & Strini, A. Weathering of granite in Antarctica: II. Thermal stress at the grain scale. *Earth Surf. Process. Landf.* **33**, 475–493 (2008).
10. Matsuoka, N. & Murton, J. Frost weathering: recent advances and future directions. *Permafr. Periglac. Process.* **19**, 195–210 (2008).
11. Jongmans, A. G. et al. Rock-eating fungi. *Nature* **389**, 682–683 (1997).
12. Mottershead, D. N., Baily, B., Collier, P. & Inkpen, R. J. Identification and quantification of weathering by plant roots. *Build. Environ.* **38**, 1235–1241 (2003).
13. Bonneville, S. et al. Plant-driven fungal weathering: Early stages of mineral alteration at the nanometer scale. *Geology* **37**, 615–618 (2009).
14. Wild, B., Gerrits, R. & Bonneville, S. The contribution of living organisms to rock weathering in the critical zone. *Npj Mater. Degrad.* **6**, 1–16 (2022).
15. Calvaruso, C. et al. Influence of forest trees on the distribution of mineral weathering-associated bacterial communities of the *Scleroderma citrinum* mycorrhizosphere. *Appl. Environ. Microbiol.* **76**, 4780–4787 (2010).
16. Collignon, C., Uroz, S., Turpault, M.-P. & Frey-Klett, P. Seasons differently impact the structure of mineral weathering bacterial communities in beech and spruce stands. *Soil Biol. Biochem.* **43**, 2012–2022 (2011).
17. Nicolitch, O., Colin, Y., Turpault, M.-P. & Uroz, S. Soil type determines the distribution of nutrient mobilizing bacterial communities in the rhizosphere of beech trees. *Soil Biol. Biochem.* **103**, 429–445 (2016).
18. Neumann, G. & Römheld, V. Root excretion of carboxylic acids and protons in phosphorus-deficient plants. *Plant Soil* **211**, 121–130 (1999).
19. Meier, I. C. et al. Root exudation of mature beech forests across a nutrient availability gradient: the role of root morphology and fungal activity. *N. Phytol.* **226**, 583–594 (2020).

20. Frey, P., Frey-Klett, P., Garbaye, J., Berge, O. & Heulin, T. Metabolic and genotypic fingerprinting of fluorescent pseudomonads associated with the Douglas Fir-*Laccaria bicolor* mycorrhizosphere. *Appl. Environ. Microbiol.* **63**, 1852–1860 (1997).
21. Grayston, S. J., Vaughan, D. & Jones, D. Rhizosphere carbon flow in trees, in comparison with annual plants: the importance of root exudation and its impact on microbial activity and nutrient availability. *Appl. Soil Ecol.* **5**, 29–56 (1997).
22. Rangel-Castro, J. I., Danell, E. & Pfeffer, P. E. A ^{13} C-NMR study of exudation and storage of carbohydrates and amino acids in the ectomycorrhizal edible mushroom *Cantharellus cibarius*. *Mycologia* **94**, 190–199 (2002).
23. Jolivet, C., Angers, D. A., Chantigny, M. H., Andreux, F. & Arrouays, D. Carbohydrate dynamics in particle-size fractions of sandy spodosols following forest conversion to maize cropping. *Soil Biol. Biochem.* **38**, 2834–2842 (2006).
24. Medeiros, P. M., Fernandes, M. F., Dick, R. P. & Simoneit, B. R. T. Seasonal variations in sugar contents and microbial community in a ryegrass soil. *Chemosphere* **65**, 832–839 (2006).
25. Hameeda, B., Reddy, Y. H. K., Rupela, O. P., Kumar, G. N. & Reddy, G. Effect of carbon substrates on rock phosphate solubilization by bacteria from composts and macrofauna. *Curr. Microbiol.* **53**, 298–302 (2006).
26. Reyes, I., Valery, A. & Valduz, Z. Phosphate-solubilizing microorganisms isolated from rhizospheric and bulk soils of colonizer plants at an abandoned rock phosphate mine. In *First international meeting on microbialphosphate solubilization*, 69–75 (Springer, Netherlands, 2007).
27. Patel, D. K., Archana, G. & Kumar, G. N. Variation in the nature of organic acid secretion and mineral phosphate solubilization by *Citrobacter* sp. DHRSS in the presence of different sugars. *Curr. Microbiol.* **56**, 168–174 (2008).
28. Suleman, M. et al. Phosphate solubilizing bacteria with glucose dehydrogenase gene for phosphorus uptake and beneficial effects on wheat. *PLoS ONE* **13**, e0204408 (2018).
29. Uroz, S. et al. Efficient mineral weathering is a distinctive functional trait of the bacterial genus *Collimonas*. *Soil Biol. Biochem.* **41**, 2178–2186 (2009b).
30. Robert, M. & Berthelin, J. Role of biological and biochemical factors in soil mineral weathering. in *SSSA Special Publications* (eds. Huang, P. M. & Schnitzer, M.) 453–495 (Soil Science Society of America, 1986).
31. Barker, W. W., Welch, S. A., Chu, S. & Banfield, J. F. Experimental observations of the effects of bacteria on aluminosilicate weathering. *Am. Mineral.* **83**, 1551–1563 (1998).
32. Kalinowski, B. E., Liermann, L. J., Brantley, S. L., Barnes, A. & Pantano, C. G. X-ray photoelectron evidence for bacteria-enhanced dissolution of hornblende. *Geochim. Cosmochim. Acta* **64**, 1331–1343 (2000).
33. Liermann, L. J., Kalinowski, B. E., Brantley, S. L. & Ferry, J. G. Role of bacterial siderophores in dissolution of hornblende. *Geochim. Cosmochim. Acta* **64**, 587–602 (2000).
34. Goldstein, A. H. Recent progress in understanding the molecular genetics and biochemistry of calcium phosphate solubilization by gram negative bacteria. *Biol. Agric. Hortic.* **12**, 185–193 (1995).
35. Illmer, P. & Schinner, F. Solubilization of inorganic calcium phosphates—Solubilization mechanisms. *Soil Biol. Biochem.* **27**, 257–263 (1995).
36. Sashidhar, B. & Podile, A. R. Mineral phosphate solubilization by rhizosphere bacteria and scope for manipulation of the direct oxidation pathway involving glucose dehydrogenase. *J. Appl. Microbiol.* **109**, 1–12 (2010).
37. Gyaneshwar, P. et al. Involvement of a phosphate starvation inducible glucose dehydrogenase in soil phosphate solubilization by *Enterobacter asburiae*. *FEMS Microbiol. Lett.* **171**, 223–229 (1999).
38. Tripura, C., Sudhakar Reddy, P., Reddy, M. K., Sashidhar, B. & Podile, A. R. Glucose dehydrogenase of a rhizobacterial strain of *Enterobacter asburiae* involved in mineral phosphate solubilization shares properties and sequence homology with other members of enterobacteriaceae. *Indian J. Microbiol.* **47**, 126–131 (2007).
39. Intorne, A. C. et al. Identification and characterization of *Gluconacetobacter diazotrophicus* mutants defective in the solubilization of phosphorus and zinc. *Arch. Microbiol.* **191**, 477–483 (2009).
40. Sashidhar, B. & Podile, A. R. Transgenic expression of glucose dehydrogenase in *Azotobacter vinelandii* enhances mineral phosphate solubilization and growth of sorghum seedlings. *Microb. Biotechnol.* **2**, 521–529 (2009).
41. Miller, S. H. et al. Biochemical and genomic comparison of inorganic phosphate solubilization in *Pseudomonas* species: Inorganic P-solubilization in *Pseudomonas*. *Environ. Microbiol. Rep.* **2**, 403–411 (2010).
42. Crespo, J. Mineral phosphate solubilization activity of *Gluconacetobacter diazotrophicus* under P-limitation and plant root environment. *Agric. Sci.* **2**, 16–22 (2011).
43. Wang, Y. L. et al. Interactions between biotite and the mineral-weathering bacterium *Pseudomonas azotoformans* F77. *Appl. Environ. Microbiol.* **86**, e02568–19 (2020).
44. Picard, L., Turpault, M.-P., Oger, P. M. & Uroz, S. Identification of a novel type of glucose dehydrogenase involved in the mineral weathering ability of *Collimonas pratensis* strain PMB3(1). *FEMS Microbiol. Ecol.* **97**, fiaa232 (2021).
45. Hersman, L., Lloyd, T. & Sposito, G. Siderophore-promoted dissolution of hematite. *Geochim. Cosmochim. Acta* **59**, 3327–3330 (1995).
46. Reichard, P. U., Kretzschmar, R. & Kraemer, S. M. Dissolution mechanisms of goethite in the presence of siderophores and organic acids. *Geochim. Cosmochim. Acta* **71**, 5635–5650 (2007).
47. Perez, A. et al. Direct and indirect impact of the bacterial strain *Pseudomonas aeruginosa* on the dissolution of synthetic Fe(III)- and Fe(II)-bearing basaltic glasses. *Chem. Geol.* **523**, 9–18 (2019).
48. Ferret, C. et al. Siderophore-promoted dissolution of smectite by fluorescent *Pseudomonas*: Smectite alteration by bacteria. *Environ. Microbiol. Rep.* **6**, 459–467 (2014).
49. Parrello, D., Zegeye, A., Mustin, C. & Billard, P. Siderophore-mediated iron dissolution from nontronites is controlled by mineral cristallochemistry. *Front. Microbiol.* **7**, 423 (2016).
50. Picard, L. et al. The mineral weathering ability of *Collimonas pratensis* PMB3(1) involves a Malleobactin-mediated iron acquisition system. *Environ. Microbiol.* **24**, 784–802 (2022).
51. Uroz, S. et al. Effect of the mycorrhizosphere on the genotypic and metabolic diversity of the bacterial communities involved in mineral weathering in a forest soil. *Appl. Environ. Microbiol.* **73**, 3019–3027 (2007).
52. Jones, D. L. Organic acids in the rhizosphere – a critical review. *Plant Soil* **205**, 25–44 (1998).
53. Welch, S. A., Taunton, A. E. & Banfield, J. F. Effect of microorganisms and microbial metabolites on apatite dissolution. *Geomicrobiol. J.* **19**, 343–367 (2002).
54. Adhikary, H., Sanghavi, P. B., Macwan, S. R., Archana, G. & Naresh Kumar, G. Artificial citrate operon confers mineral phosphate solubilization ability to diverse fluorescent Pseudomonads. *PLoS ONE* **9**, e107554 (2014).
55. Goyne, K. W., Brantley, S. L. & Chorover, J. Rare earth element release from phosphate minerals in the presence of organic acids. *Chem. Geol.* **278**, 1–14 (2010).
56. Lin, Q. et al. Effect of low-molecular-weight organic acids on hematite dissolution promoted by desferrioxamine. *B. Environ. Sci. Pollut. Res.* **25**, 163–173 (2018).
57. Uroz, S., Calvaruso, C., Turpault, M.-P. & Frey-Klett, P. Mineral weathering by bacteria: ecology, actors and mechanisms. *Trends Microbiol.* **17**, 378–387 (2009a).
58. Uroz, S. et al. Dual transcriptomics and proteomics analyses of the early stage of interaction between *Caballeronia mineralivorans* PML1(12) and mineral. *Environ. Microbiol.* **22**, 3838–3862 (2020).
59. Uroz, S., Picard, L. & Turpault, M.-P. Recent progress in understanding the ecology and molecular genetics of soil mineral weathering bacteria. *Trends Microbiol.* **30**, 882–897 (2022).
60. Sasnow, S. S., Wei, H. & Aristilde, L. Bypasses in intracellular glucose metabolism in iron-limited *Pseudomonas putida*. *MicrobiologyOpen* **5**, 3–20 (2016).
61. Mendonca, C. M. et al. Hierarchical routing in carbon metabolism favors iron-scavenging strategy in iron-deficient soil *Pseudomonas* species. *Proc. Natl Acad. Sci. USA* **117**, 32358–32369 (2020).
62. Nicolitch, O. et al. A microcosm approach highlights the response of soil mineral weathering bacterial communities to an increase of K and Mg availability. *Sci. Rep.* **9**, 14403 (2019).
63. Lepleux, C., Turpault, M. P., Oger, P., Frey-Klett, P. & Uroz, S. Correlation of the abundance of betaproteobacteria on mineral surfaces with mineral weathering in forest soils. *Appl. Environ. Microbiol.* **78**, 7114–7119 (2012).
64. Colin, Y., Nicolitch, O., Turpault, M.-P. & Uroz, S. Mineral types and tree species determine the functional and taxonomic structures of forest soil bacterial communities. *Appl. Environ. Microbiol.* **83**, e02684–16 (2017).
65. Bryce, C. C. et al. Rock geochemistry induces stress and starvation responses in the bacterial proteome: rock-driven changes in the bacterial proteome. *Environ. Microbiol.* **18**, 1110–1121 (2016).
66. Liu, C. et al. The *eno* gene of *Burkholderia cenocepacia* strain 71-2 is involved in phosphate solubilization. *Curr. Microbiol.* **76**, 495–502 (2019).
67. Wang, Y.-L. et al. A combination of genomics, transcriptomics, and genetics provides insights into the mineral weathering phenotype of Pseudomonas azotoformans F77. *Appl. Environ. Microbiol.* **87**, e01552–21 (2021).
68. Hutchens, E., Valsami-Jones, E., McEldowney, S., Gaze, W. & McLean, J. The role of heterotrophic bacteria in feldspar dissolution – an experimental approach. *Mineral. Mag.* **67**, 1157–1170 (2003).
69. Dehner, C. A., Awaya, J. D., Maurice, P. A. & DuBois, J. L. Roles of siderophores, oxalate, and ascorbate in mobilization of iron from hematite by the aerobic bacterium *Pseudomonas mendocina*. *Appl. Environ. Microbiol.* **76**, 2041–2048 (2010).
70. Perez, A. et al. Bioalteration of synthetic Fe(III)-, Fe(II)-bearing basaltic glasses and Fe-free glass in the presence of the heterotrophic bacteria strain *Pseudomonas aeruginosa*: Impact of siderophores. *Geochim. Cosmochim. Acta* **188**, 147–162 (2016).
71. Blanco Nouche, C. et al. The Non-ribosomal peptide synthetase-Independent Siderophore (NIS) Rhizobactin produced by *Caballeronia mineralivorans* PML1(12) confers the ability to weather minerals. *Appl. Environ. Microbiol.* (2023).

72. Harrington, J. M. et al. Structural dependence of Mn complexation by siderophores: donor group dependence on complex stability and reactivity. *Geochim. Cosmochim. Acta* **88**, 106–119 (2012).
73. Zhang, L. et al. Bioleaching of rare earth elements from bastnaesite-bearing rock by actinobacteria. *Chem. Geol.* **483**, 544–557 (2018).
74. Valbi, V., Perez, A., Verney-Carron, A. & Rossano, S. Impact of a Mn-oxidizing bacterial strain on the dissolution and browning of a Mn-bearing potash-lime silicate glass. *npj Mater. Degrad.* **7**, 20 (2023).
75. Olsson-Francis, K., Van Houdt, R., Mergeay, M., Leys, N. & Cockell, C. S. Microarray analysis of a microbe-mineral interaction: Analysis of a microbe-mineral interaction. *Geobiology* **8**, 446–456 (2010).
76. Liu, H., Liu, X., Li, X., Fu, Z. & Lian, B. The molecular regulatory mechanisms of the bacteria involved in serpentine weathering coupled with carbonation. *Chem. Geol.* **565**, 120069 (2021).
77. Calvaruso, C., Turpault, M. P., Frey-Klett, P., Uroz, S., Pierret, M. C., Tosheva, Z. & Kies, A. Increase of apatite dissolution rate by Scots pine roots associated or not with Burkholderia glathei PML1 (12) Rp in open-system flow microcosms. *Geochim. Cosmochim. Acta* **106**, 287–306 (2013).
78. Picard, L., Oger, P., Turpault, M.-P. & Uroz, S. Draft genome sequence of *Collimonas pratensis* strain PMB3(1), an effective mineral-weathering and chitin-hydrolyzing bacterial strain. *Microbiol. Resour. Announc.* **9**, e00601–20 (2020).
79. Chilton, M.-D. et al. *Agrobacterium tumefaciens* DNA and PS8 bacteriophage DNA not detected in crown gall tumors. *Proc. Natl Acad. Sci. USA* **71**, 3672–3676 (1974).
80. Schwyn, B. & Neilands, J. B. Universal chemical assay for the detection and determination of siderophores. *Anal. Biochem.* **160**, 47–56 (1987).

ACKNOWLEDGEMENTS

This work was supported by grants from the EC2CO and Laboratory of Excellence Arbre (ANR-11-LABX-0002-01) programs to S.U. L.P. was supported by a fellowship from the French Ministère de l'Enseignement Supérieur, de la Recherche et de l'Innovation and C.B.N was supported by a fellowship from INRAE and the Lorraine Region. The UMR1136 and UR1138 are supported by the ANR through the Laboratory of Excellence Arbre (ANR-11-LABX-0002-01). We thank the editor and the 2 reviewers that permitted to improve the manuscript.

AUTHOR CONTRIBUTIONS

Conceptualization: S.U., M-P.T.; Conducted experiment: L.P., C.B.N., C.C.; Formal analysis: L.P., M-P.T., S.U.; Methodology: L.P., M-P.T., S.U. ; Writing—original draft: L.P., M-P.T., S.U.; Writing—review & editing: L.P., C.B.N., M-P.T., S.U.

COMPETING INTERESTS

The authors declare no competing interests.

ADDITIONAL INFORMATION

Supplementary information The online version contains supplementary material available at https://doi.org/10.1038/s41529-023-00396-9.

Correspondence and requests for materials should be addressed to Stéphane Uroz.

Reprints and permission information is available at http://www.nature.com/reprints

Publisher's note Springer Nature remains neutral with regard to jurisdictional claims in published maps and institutional affiliations.

Open Access This article is licensed under a Creative Commons Attribution 4.0 International License, which permits use, sharing, adaptation, distribution and reproduction in any medium or format, as long as you give appropriate credit to the original author(s) and the source, provide a link to the Creative Commons license, and indicate if changes were made. The images or other third party material in this article are included in the article's Creative Commons license, unless indicated otherwise in a credit line to the material. If material is not included in the article's Creative Commons license and your intended use is not permitted by statutory regulation or exceeds the permitted use, you will need to obtain permission directly from the copyright holder. To view a copy of this license, visit http://creativecommons.org/licenses/by/4.0/.

© The Author(s) 2023